Molecular recognition of lipopolysaccharide by the lantibiotic nisin

By:

Alice BM Lanne[1], Alice Goode[1], Charlotte Prattley[1], Divya Kumari[1], Mette Ryun Drasbek[3], Paul Williams[2], Raquel Conde-Álvarez[4], Ignacio Moriyón[4] & Boyan B. Bonev[1*]

From:

[1] School of Life Sciences, QMC, University of Nottingham, Nottingham NG7 2UH, UK

[2] Centre for Biomolecular Sciences, University of Nottingham, Nottingham NG7 2RD, UK

[3] DuPont Nutrition Biosciences ApS. Edwin Rahrs Vej 38, DK-8220 Brabrand, Denmark

[4] Instituto de Salud Tropical, Instituto de Investigación Sanitaria de Navarra, and Departamento de Microbiología y Parasitología, Universidad de Navarra, c/Irunlarrea 1, 31008 Pamplona, Spain.

[*] Correspondence: boyan.bonev@nottingham.ac.uk

Abstract

Nisin is a lanthionine antimicrobial effective against diverse Gram-positive bacteria and is used as a food preservative worldwide. Its action is mediated by pyrophosphate recognition of the bacterial cell wall receptors lipid II and undecaprenyl pyrophosphate. Nisin/receptor complexes disrupt cytoplasmic membranes, inhibit cell wall synthesis and dysregulate bacterial cell division. Gram-negative bacteria are much more tolerant to antimicrobials including nisin. In contrast to Gram-positives, Gram-negative bacteria possess an outer membrane, the major constituent of which is lipopolysaccharide (LPS). This contains surface exposed phosphate and pyrophosphate groups and hence can be targeted by nisin. Here we describe the impact of LPS on membrane stability in response to nisin and the molecular interactions occurring between nisin and membrane-embedded LPS from different Gram-negative bacteria. Dye release from liposomes shows enhanced susceptibility to nisin in the presence of LPS, particularly rough LPS chemotypes that lack an O-antigen whereas LPS from microorganisms sharing similar ecological niches with antimicrobial producers provides only modest enhancement. Increased susceptibility was observed with LPS from pathogenic *Klebsiella pneumoniae* compared to LPS from enteropathogenic *Salmonella enterica* and gut commensal *Escherichia coli*. LPS from *Brucella melitensis*, an intra-cellular pathogen which is adapted to invade professional and non-professional phagocytes, appears to be refractory to nisin. Molecular complex formation between nisin and LPS was studied by solid state MAS NMR and revealed complex formation between nisin and LPS from most organisms investigated except *B. melitensis*. LPS/nisin complex formation was confirmed in outer membrane extracts from *E. coli*.

Introduction

The rise in antimicrobial resistance (AMR) poses a significant global threat to the management of infectious diseases. Gram-negative pathogens are particularly problematic, as emerging resistance to last-line drugs has been reported [1] and they constitute all of the entries to the WHO AMR critical pathogen priority list [2]. In addition to the threat posed by AMR, control of food related Gram-negative bacteria is an essential component of global food security [3]. A key feature of Gram-negative bacteria contributing to AMR is the presence of an outer membrane (OM) permeability barrier that protects peptidoglycan and other intracellular targets from antibiotics and other antimicrobials.

Bacterial outer membranes are asymmetric protein embedded bilayers with phospholipid inner leaflets and lipopolysaccharide (LPS) outer leaflets. The OM defines bacterial interactions with the host and the environment and acts as a selectivity barrier with a key role in molecular uptake [4]. The OM protects bacteria from environmental noxious molecules including many antibiotics [5] and modulates susceptibility to cationic antimicrobial peptides [6].

LPS molecules commonly contain three regions: a conserved hexa- or hepta-acyl disaccharide, lipid A, which acts as a hydrophobic anchor to the membrane; a core oligosaccharide, which can be further subdivided into the conserved inner region and variable outer core; and, a specific O-antigen that varies greatly between species [5]. LPS containing all 3 components confers a ‘smooth’ surface phenotype, while mutants lacking an O-antigen and sometimes parts of the inner core result in chemotypes that present as rough bacterial colony phenotypes.

LPS shows structural variation between bacterial species with highest degree of similarity within the lipid A region and species- or serotype-specificity contained in the outer core and O-antigen. Most lipid A structures contain a (1-6)-linked glucosamine disaccharide backbone, which is acylated with chains that vary in length and number depending on species and is usually phosphorylated at positions 1 and 4' [7] or sometimes carrying pyrophosphorylethanolamine (Figure 1A) [8]. However, some bacteria present a different lipid A chemotype. For example, one important and distinctive feature of lipid A in the *Brucellae* is the presence of a diaminoglucose backbone carrying very long, mostly 28-carbon chains, hydroxylated at the penultimate methylene (Figure 1A) (Moreno *et al.* 1990, Iriarte, Gonzalez et al. 2004) . Such C28 chains have the correct length and hydrophilic termination to traverse both leaflets of the OM and can enhance bilayer stability as observed for archaeal membranes containing prenylated lipids.

Covalently linked to Lipid A, the core region is a short oligosaccharide composed of up to 15 sugars. The core region shows species variation with only one common structural element; 3-Deoxy-D-*manno*-oct-2-ulosonic acid (KDO), which links the core region to Lipid A [10]. KDO is often linked to several heptose residues with additional phosphate or sulfate groups but some bacteria lack core heptose [10–12]. The outer core varies more between species and consists of common hexose and hexosamine sugars [13]. Recently, we have shown that the outer core from *E. coli* rough-type C LPS is both phosphorylated and pyrophosphorylated [8]. The structural composition of LPS core in *Klebsiella pneumoniae* [14], *Escherichia coli* [12] and *Brucella melitensis* [15,16], is shown in Figure 1B.

The O-antigen displays structural diversity in both sugar composition and connectivity, which imparts an immunological fingerprint to bacteria. It is an antigenic polysaccharide formed of up to

40 repeating oligosaccharide units, predominantly neutral and basic hexose residues [13]. The O-antigen is the least conserved region of LPS, with over 190 chemotypes in *E. coli* alone [17].

LPS is shed from the OM as endotoxin during cell division and activates the host immune response through Toll-like receptor 4, TLR4 [18]. LPS-binding protein (LPB) and CD-14-MD-2 are also involved in receptor activation by LPS [19,20]. Receptor recognition of LPS shows some species specificity, often correlating with the ecological niche occupied by the species. LPS from some commensal species possess much weaker receptor binding than some pathogenic species [21]. Some bacterial pathogens exploit reduced LPS receptor recognition as a method of immune evasion [22,23].

As well as TLR4 activation, LPS makes essential receptor-independent interactions with host cell membranes. We have previously shown that cholesterol in lipid rafts plays an important role in LPS recognition, with LPS binding at higher affinity within lipid raft models. This has also been demonstrated in live cell experiments, with a reduction in LPS binding to Jurkat T-lymphocyte membranes upon cholesterol removal [24]. This receptor-independent binding of LPS to cholesterol also varies with the ecological niche of species, with the LPS of commensal organisms showing significantly weaker binding to membranes than that of many pathogens [24].

Although the OM can be a major obstacle to antibiotic delivery, LPS also presents a specific target for antimicrobials, which use LPS as receptor to gain entry into bacteria to access peptidoglycan or other intracellular targets. An example of this is colicin N, which unlike other colicins targets Gram-negative species *via* molecular recognition of a specific pyrophosphate binding epitope in the LPS outer-core [8]. An alternate approach is the use of LPS as a direct target for antimicrobial activity. For example, polymyxin B binds LPS directly *via* electrostatic interactions and penetrates via a self-

promoted mechanism, resulting in extensive OM damage and inner membrane depolarisation [25,26]. There are also antimicrobials with high LPS binding affinity that reduce the biological effects of this molecule. For example, proanthocyanidins [27,28] and polyamines such as spermine [29] are both compound classes with demonstrated high-affinity binding to the lipid A moiety of LPS. In binding lipid A, these compounds hamper LPS interactions with the mammalian receptors TLR4/MD2, and thereby reduce activation of the innate immune response and septic shock.

Some antimicrobial peptides are naturally produced by bacteria to overcome competition for space and nutrients [30]. They have been recognised as a promising alternative to antibiotics for overcoming AMR [31], and are considered safe for use as food preservatives [32]. The lantibiotic nisin is an antimicrobial peptide produced by *Lactococcus lactis*. It is a widely-used food preservative (E234) as it displays high antimicrobial activity against diverse Gram-positive bacteria [33]. The positively charged nisin binds to bacterial membranes [34] and targets pyrophosphates in the cell wall intermediates lipid II [35,36] and undecaprenyl pyrophosphate (11PP) [37]. This results in breach of the cell membrane, inhibition of cell wall synthesis and disruption of cell division and morphogenesis [38].

Here we hypothesize that phosphorylation and pyrophosphorylation sites on LPS present binding epitopes for nisin. This would be in agreement with previous studies that have shown nisin to display antimicrobial activity against certain Gram-negative species [39–41]. We studied dye release from LPS-containing liposomes to assess the role of LPS as a membrane receptor and its effect on membrane stability to nisin. Direct interactions between LPS and nisin were investigated using high resolution ^{31}P MAS solid-state NMR. We compared smooth LPS from several different Gram-negative species inhabiting different ecological niches including *B. melitensis*, an immunosilent pathogen, *K. pneumoniae*, a pulmonary pathogen and the enteric commensal *E. coli*,

that have evolved alongside enteric microbiota producing antimicrobials and under immune surveillance from the host. We also tested LPS from rough chemootypes of *E. coli*, Rc having the outer core and Rd, in which the outer core is absent, to assess the role of phosphate exposure in mutated LPS and the protective role of the O-chain.

MATERIALS AND METHODS

The phospholipid 1,2-dioleoyl-*sn*-glycero-3-phosphocholine (DOPC) (Avanti Polar Lipids Inc. Alabastar, Alabama, USA) was used as purchased at > 98% purity. LPSs from rough *E. coli* Rd and Rc chemotypes were purchased at > 99% purity from Sigma Aldrich (Poole, UK) and used without further purification. Smooth type LPSs from *K. pneumoniae* ATCC 15380, *S. enterica* and *E. coli* 111:B4 (smooth-type) were purchased at 40 – 60 % purity from Sigma Aldrich (Poole, UK) and purified as previously described [11]. LPS from *B. melitensis* was prepared in-house by phenol extraction and purified to >99% purity as described previously [42]. All other chemicals were of analytical or reagent grade. Nisin A was purified from Nisaplin (DuPont Health Bioscience ApS) to HPLC grade at >98% purity, as described previously [37,38].

LPS suspension preparation

Purified LPS was resuspended in HPLC grade water at 5 mg/ml, followed by incubation at 56°C for 15 min, vortexing for 2 min and cooling on ice. This process was repeated a total of three times. The suspension was stored at 4°C for up to 4 h. Dry lipid was hydrated with the LPS suspensions, subjected to a further three thermal cycles and liposomes recovered from centrifugation pellet as described previously [11].

Bacterial OM isolation

Cultures of *E. coli* BL21 were grown on Luria Bertani nutrient broth to OD of 1.2. Cells were pelleted by centrifugation at 4,500 x *g*, pellets were resuspended in Tris buffered saline (TBS), pH 7.5 and mechanically disrupted using 36,000 psi cell in a French press. Unbroken cells and debris were removed by centrifugation at 10,000 x *g* and the supernatant was treated with lysozyme. OMs were collected by ultracentrifugation at 100,000 x *g*, the pellet obtained was resuspended in HEPES buffer pH 7.5 and separated by sucrose gradient centrifugation.

Preparation of liposomes for leakage studies

Dry lipid films (0.2 mg DOPC) were hydrated in 1 ml 5(6)-carboxyfluorescein (CF) (Acros organics) buffer (50 mM CF, 50 mM NaCl, 10 mM Hepes, pH 7.4), for 1 h. For DOPC lipid films requiring LPS addition, 0.2 ml of a 1 mg/ml LPS suspension was added prior to CF addition and lyophilised overnight. The solution then underwent five cycles of freeze-thawing in which it was frozen with liquid nitrogen and thawed at 40°C. The solution was extruded 11 times through a 1 μm pore size polycarbonate filter using an Avanti extruder (Avanti polar lipids Inc). The excess CF was removed by gel filtration on a PD-10 column (GE Healthcare) equilibrated with 100 mM NaCl in 10 mM Hepes, pH 7.4. The CF labelled vesicles were collected, stored a 4°C, and used within 24 h.

Dye release studies

Pure nisin was dissolved in 100 mM NaCl, 10 mM Hepes (pH 7.4) and equilibrated overnight at 4°C. Nisin-induced CF release was monitored by measuring fluorescence increase (excitation 490 nm, emission 515 nm, 400 V) over 240 s, at which time intensity changes with time were within 1%. CF-loaded large unilamellar vesicles (LUVs) in buffer (100 mM NaCl, 10 mM Hepes, pH 7.4) were equilibrated until steady background fluorescence was achieved, as described previously [43]. Nisin was added after 60 s (final concentration range of 50 – 0.75 μg/ml) and after equilibration residual liposomes were dispersed with Triton X-100 (Fluka Biochemika). The procedure was

repeated in triplicate for all vesicles at all nisin concentrations. The peptide-induced CF leakage was expressed as a fraction of CF release on Triton X-100 addition, normalised to background fluorescence:

$$\% \text{ leakge} = (F_{nisin} - F_0)/(F_{Tx} - F_0)*100$$

where F_0 is the baseline fluorescence recorded before addition of nisin, F_{nisin} is the steady state fluorescence induced by nisin and F_{Tx} is the maximum fluorescence after Triton X-100 addition.

Solid state NMR

All experiments were performed on a Varian VNMRS400 widebore spectrometer with a 4 mm T3 MAS NMR probe (Varian, Palo Alto CA, USA). Temperature was regulated using balanced heated/vortex tube-cooled gas flow [44]. All ^{31}P MAS NMR spectra were referenced externally to 10% H_3PO_4 at 0 ppm. Direct excitation spectra were obtained using a single 125 kHz pulse, followed by proton decoupling. Heteronuclear SPINAL-64 proton decoupling [45] of 45 kHz B_1 was sufficient to remove heteronuclear interactions, as phosphates have no directly bonded protons and two-bond couplings are comparatively weak. Spectral acquisitions were repeated at 5 s interpulse delay during direct excitation experiments, which exceeds approximately five-fold the ^{31}P and ^{1}H longitudinal relaxation times in lipids and 8192 transients were averaged in each acquisition. All experiments were acquired at 5 kHz MAS speed and 20°C, unless otherwise stated. Spectra were processed and analysed using ACD/Labs (Advanced Chemistry Development, Inc., Toronto, Canada). Spectral deconvolution was used for the quantitative analysis of spectra and cumulative pyrophosphate fractional intensity was used to estimate the molar fraction of LPS in the membranes, as previously described [34,46]. Chemical shifts were compared to spectral simulations for 1,4 phosphorylation or pyrophosphorylation of each monosaccharide, according to

published values. Homogeneous broadening was assumed and resonances were approximated by fitting Gauss-Lorentzian lineshapes with 5 Hz Lorentzian broadening.

RESULTS

LPS modulates nisin-induced dye release

The role of LPS as a receptor for nisin is reflected in the extent to which its presence in model membranes modulates nisin-induced dye release. LUVs of DOPC containing 1:1 w:w LPS (between 2 and 12% molar, depending on LPS type) were used as membrane mimics, as the zwitterionic phosphatidylcholine (PC) headgroups only show weak, non-specific interactions with nisin [34].

CF release from pure DOPC vesicles was used as negative control and compared with leakage from DOPC vesicles containing LPS from different Gram-negative species. Changes in fluorescence are reported from steady state, reached after equilibration. In all cases, the similar levels of CF release (typically monitored at 20% and 40% release) were observed from LPS-containing liposomes at lower nisin/lipid ratios compared with pure DOPC (Figure 2). This increase in leakage was chemotype and bacterial species dependent, with rough-type LPS mutants of *E. coli* (Rd) and (Rc) causing the highest increases in sensitivity to nisin. Dye release was bimodal with weaker dose-response at low levels of nisin (typically below 20% release) followed by stronger dose-response beyond a break in trend (typically near 40% release), in which dose-response becomes parallel to that in LPS-free liposomes. Low level leakage is dominated by initial LPS recognition and leads to partial dye release, which is reflected in levelling of the response to increasing nisin concentrations after available LPS sites are occupied. This initial nisin release is enhanced significantly in the presence of LPS. The high level regimen is dominated by receptor-independent breach of the DOPC bilayer by nisin, in which DOPC/nisin interactions are responsible for membrane instability which lead to total dye release. The high levels of leakage are characterised by a faster dye release

with a stronger response to nisin at higher concentrations (typically near and above 40% dye release) and is identifiable in all leakage curves. Within this regimen, dose-response is very similar in the absence and presence of all LPS types.

To understand the role of LPS as a receptor for nisin we followed the low levels of CF release up to 20 or 30%. The presence of rough chemotype LPS from *E. coli* enhanced membrane disruption approximately 20-fold, compared to pure DOPC vesicles (Figure 2). Smooth type LPS from *K. pneumoniae* also enhanced sensitivity to nisin with LPS from both species resulting in 20% CF release occurring at fivefold lower nisin concentrations than PC vesicles. LPS from *E. coli*, smooth chemotype, *S. enterica* and *B. melitensis* had a weaker effect on nisin-induced leakage with 3 to 2-fold lower nisin/DOPC levels at 20 % CF release compared to DOPC membranes. Initial release at <10% CF leakage singles out LPS from *B. melitensis*, in the presence of which membrane stability was maintained better than the other LPS types. In addition to differences in the core, this difference can be rationalised when considering enhanced membrane stability in the presence of the C28-OH chain in *B. melitensis* LPS (Figure 1), which is absent from all other LPS chemotypes.

We compared the effects that individual LPS types have on membrane susceptibility to nisin by considering dye release at different nisin/LPS molar ratios (Figure 3). While the molecular weight for rough types LPS are known, the molecular weight for the smooth LPS types were calculated from the ^{31}P MAS NMR spectra using the fractional intensity of the pyrophosphates (*cf.* the NMR section below). Direct comparison of dye release in the presence of different LPSs confirmed that rough chemotypes sensitize membranes to nisin to a greater extent than smooth chemotypes and at 20% CF release, the membrane leakage was enhanced in descending order from *E. coli* Rd and Rc, smooth chemotype *K. pneumoniae*, *E. coli*, and *S. enterica* with the least impact observed in the presence of *B. melitensis* LPS. Compared to *B. melitensis* and *S. enterica* LPS, rough chemotype

E. coli Rd and Rc LPS show 20 and 10-fold leakage enhancement respectively, followed by *K. pneumoniae*, and *E. coli* at 3 to 2-fold. At this level of dye release, the protective effect of C28-OH was overwhelmed and membranes with LPS from *E. coli* and *S. enterica*, two bacterial species that are well-adapted to antimicrobials produced by gut microbiota [47],responded in a comparable way to membranes containing LPS from *B. melitensis*. Similarity in the lipid A region dictates common responses to nisin for all smooth LPS chemotypes. Rough chemotypes stood out, which clearly demonstrate the protective role of the O-antigen and the outer core as observed in the different responses noted for *E. coli* smooth, Rd and Rc chemotypes.

Molecular interactions and nisin/LPS membrane complexes – solid state NMR studies

In some bacteria, the core region of LPS can be phosphorylated and/or pyrophosphorylated [4,11], which provides unique reporters for studying molecular interactions in membranes by solid state NMR [24]. We used high resolution solid state ^{31}P MAS NMR to observe changes in the spectroscopic fingerprints of LPSs which are caused by changes in electronic environment of negatively charged phosphates following interactions with the cationic lantibiotic nisin. We consider two possibilities: a change in ionization state from RPO_4^{2-} to $RHPO_4^-$, which carries a significant downfield shift of approximately -1ppm; and a redistribution of electron density in the proximity of the cationic peptide, which leads to more subtle changes in isotropic chemical shifts [48]. To understand the molecular bases of different membrane tolerances to nisin in the presence of LPS from different microorganisms, we considered *B. melitensis* LPS, which caused very little change, *E. coli* LPS, which did reduce nisin tolerance to a small extent and, *K. pneumoniae* smooth LPS, which enhanced most significantly membrane susceptibility to nisin. In addition, we considered rough chemotype LPS from *E. coli* to understand the role of O-antigen as an accessibility barrier, as well as *E. coli* OM extracts to bring our models to a closer approximation of the membrane environment in bacterial cells.

Dye release showed minimal impact of smooth type LPS from *B. melitensis* on DOPC membrane stability. Membranes of the same composition, *B. melitensis* LPS/DOPC in 1:1 w/w ratio, were studied by high resolution ^{31}P MAS NMR. The spectrum is dominated by the DOPC phosphate resonance at -0.97ppm and no additional phosphates were observed (Figure 4a). A single, well-resolved pyrophosphate resonance from the LPS is seen at -11.6ppm. The overlapping resonances from the two phosphorus signals reveal that the PP is alkylated (amino-alkylated) and not free, consistent with genomic predictions and mutant analyses [49]. Comparing the integrals of the two resonances allowed us to estimate the molar ratio at approximately 2% and Mw at 39.3 ±0.2 kDa, which was used in Figure 3. Addition of nisin lead to a small downfield shift in PP to -11.4 ppm, which we interpret as the result of changes in surface charge density, rather than a specific molecular interaction [48].

The presence of LPS from *K. pneumoniae* shows the highest degree of increase in membrane susceptibility to nisin. To understand better the molecular bases of this observation we investigated LPS/DOPC membranes at 1:1 w/w ratio by ^{31}P MAS NMR (Figure 4b). DOPC molar excess yields the dominant intensity at -0.97 ppm but the phosphorylation pattern of *K. penumoniae* LPS is significantly different from that of *B. melitensis* (*cf.* Figure 4a). Pyrophosphorylation is evident with resonances at -6.8 and -12.2 ppm alongside well-resolved phosphate at 2.0 ppm, a phosphate 3.4 ppm (derived from spectral fitting) and phosphonate at 19.6 ppm, as we previously reported [11] (Figure 4b). Integral intensities in the pyro- and monophosphates relate approximately as 1:1:1:2:1 in increasing chemical shift. The phosphonate intensity is significantly smaller, due to high mobility in the phosphorylated region. Comparison with the DOPC intensity yields an estimate for the molar fraction at 2.0% and M_w of 40.1 ±0.2 kDa for *K. pneumoniae* LPS.

The single pyrophosphate is non-alkylated with the resonance at -10.7 ppm arising from the proximal to the saccharide phosphate at position 4 on glucose (predicted shift of -10.7 ppm) and a free distal phosphate at -6.8 ppm, which revealed a charge of -2 (predicted shift was -6.5 ppm for RPO_4^{2-} and for charge of -1 in $RHPO_4^-$ was -8.0 ppm).

Addition of nisin lead to a minor downfield shift in both pyrophosphate resonances, more pronounced in the distal, free phosphate from -6.8 to -7.1 ppm and in the proximal phosphate from -12.2 to -12.3 ppm (Figure 4b, bottom). The comparatively small change suggests charge density redistribution due to proximity of nisin [48], rather than a change in phosphate ionization state. The LPS phosphates showed a significantly stronger response, in which the 3.4 ppm resonance is no longer observable, while the major resonance at 2.0 ppm is shifted to 1.1 ppm. The resonance at 3.4 ppm corresponds to a doubly ionized 4-heptose monophosphate, while the 2.0→1.1 ppm shift is interpreted as protonation of 1-Hep phosphate. These observations point to a binding site for nisin between the inner and outer core of *K. pneumoniae* LPS.

The phosphonate chemical shift remained unchanged but the resonance gained intensity following nisin binding which leads to increased efficiency of proton decoupling. While not involved directly in the interaction with nisin, the phosphorylation site is close and dynamically coupled to the LPS binding site.

DOPC membranes containing an equal weight of LPS from smooth chemotype *E. coli* were slightly more susceptible to nisin than membranes containing LPS from *B. melitensis* or *S. enterica* but more resistant than membranes containing *K. penumoniae* LPS (Figure 3). Solid state ^{31}P MAS NMR spectra from *E. coli* smooth LPS-containing membranes showed a single site of non-alkylated

pyrophosphorylation with proximal phosphate resonance at -10.8 ppm and distal free doubly ionized phosphate at -5.9 ppm (Figure 4c). A phosphate resonance from *E. coli* smooth LPS was observed at 3.2 ppm with twice the intensity of the individual phosphates in the pyrophosphates spectral features. Mean integral comparison of pyrophosphate resonances with the dominant DOPC phosphate resonance at -0.97 ppm showed LPS to be present at 2.2 molar % and an approximate M_w of 35.7 ±0.2 kDa.

Addition of nisin had a profound effect on the monophosphate resonance shift, which changed by -0.9 ppm from 3.2 to 2.3 ppm. In addition, the distal phosphate resonance in the pyrophosphate was shifted by -0.3 ppm from -5.9 to -6.2 ppm. The proximal to the saccharide phosphate was only slightly shifted from -10.7 to -10.8 ppm, as it is further away from the cationic peptide and screened by electronic distribution of the distal phosphate. The large chemical shift change in the monophosphate resonance revealed its direct involvement in the binding site for nisin and a change in its protonation state following nisin binding.

Since rough chemotypes lack O-chain protection such that the core region is more easily accessible to antimicrobials [8], we investigated the role of phosphates in Rc LPS from *E. coli* in nisin binding by following changes in the high-resolution ^{31}P MAS NMR spectra from Rc LPS in DOPC membranes. The pyrophosphorylation is different from that for the smooth chemotype [8], showing that the majority of pyrophosphates are not free but alkylated, as seen in the chemical shift values of -10.7 and -11.5 ppm (Figure 5a). Addition of nisin appeared to affect neither pyrophosphate shifts, nor their relative intensity, which lead us to the conclusion that the alkylated pyrophosphates do not participate in nisin binding.

The Rc LPS is multiply phosphorylated as seen in resonances at 0.2 and -0.5 ppm with fractional intensities of 25 and 26%, respectively (Figure 5a). An additional resonance of 3.6% spectral contribution is resolved at -1.8 ppm. Addition of nisin attenuated slightly the resonance at -0.5 ppm and more significantly the 0.1 ppm resonance from 25% to 7%. Nisin binding also revealed an additional resonance at 0.6 ppm, the intensity of which is likely to have been reduced by segmental motions in nisin-free LPS.

Rough LPS phenotype d (Rd) lacks the outer core region, which contains a number of important phosphorylation and pyrophosphorylation sites [8]. Equal fractions by weight of *E. coli* Rd LPS in DOPC membranes contribute little to ^{31}P MAS NMR intensity. A free pyrophosphate is observed at -12.3 and -7.4 ppm for the proximal and distal phosphates with a contribution of 1% along with monophosphates at 1.7 and 2.6 ppm of 1% intensity each (Figure 5b). The free pyrophosphate is likely located at position 1 or 4' on the glucosamine disaccharide of lipid A and can also be resolved in the spectra from Rc LPS in representative small contribution [8]. Addition of nisin shifted the distal pyrophosphate resonance from -7.4 to -8.1 ppm, which was accompanied by a small shift of the proximal one from -12.3 to -12.5 ppm while the relative resonance intensity remained unchanged. The monophosphate resonances coalesced into a single peak at 1.26 ppm with intensity of 2% relative to DOPC.

Comparison between the ^{31}P NMR spectra from Rc and Rd LPS (Figure 5) shows significantly greater degree of phosphorylation and pyrophosphorylation in Rc LPS compared to Rd LPS from *E. coli*. A direct indicator is the lipid A resonance at -12.3 ppm, present in both spectra but at very low intensity in the NMR spectrum from Rc LPS compared to pyrophosphates form the outer core. This is a significant observation, which reveals the outer core of LPS as the primary site for

phosphorylation and pyrophosphorylation rather than lipid A and points to the key contribution of the outer core to divalent cation coordination and as the LPS layer stability mediator.

To bridge our model studies with the effect of nisin on bacterial envelopes *in situ* we investigated OM extracts from *E. coli* BL21 using ^{31}P solid state MAS NMR (Figure 6). This strain has rough type LPS lacking the O-antigen and its ^{31}P NMR spectroscopic features compare with those from Rc LPS (Figure 5a). Significant pyrophosphorylation is evident with species giving rise to major resonances at -10.8 and -12.9 ppm with relative intensity of 29 and 6%, respectively. The resonances are significantly broader in these primarily composed of LPS membranes than in the LPS/DOPC membranes, where collective effects are removed by electrostatic repulsion between LPS molecules (Figure 4c). A monophosphate resonance is seen at 3.3 ppm (Figure 6) corresponds to the 3.2 ppm resonance in LPS from smooth chemotype *E. coli* (*cf.* Figure 4c). Addition of nisin lead to comparatively small changes in the pyrophosphate region, where the -12.3 ppm resonance was shifted to -12.9 ppm without any marked change in relative intensity between the two peaks. However, as in the smooth type LPS chemotype, the upfield phosphate resonance at 3.3 ppm was suppressed entirely or shifted downfield to merge with another resonance at final shift of 1.6 ppm (Figure 6).

DISCUSSION

Nisin acts against Gram-positive bacteria through binding pyrophosphates on bacterial cell wall precursors lipid II and 11PP [35,37] to form pores in the cell membrane, disrupting the membrane and inhibiting cell wall synthesis [36]. Although in Gram-negative bacteria the peptidoglycan precursors are protected by the OM, previous work has revealed phosphorylation and pyrophosphylation of LPS [8,11], which together with divalent cations are essential for OM stability, (Nikaido 2003)[1] [4] but can also serve as receptors on the bacterial surfaces. Such

receptor binding sites can be utilised by antimicrobial proteins and peptides for destabilising and traversing the OM, as we have shown to occur during the action of colicin N (Johnson, Ridley et al. 2014)[2] [8]**,** which was also corroborated by the reported activity of nisin against Gram-negative bacteria treated with metal ion chelators [50]. Here, we observed for the first time that LPS can form molecular complexes with nisin which can destabilise membranes and that such complexes form in model membranes, as well as in bacterial OM extracts. The degree, to which LPS mediates membrane disruption by nisin is influenced by the bacterial origin of the LPS and is related to the ecological life style of the bacterial species.

Activation of host TLR4-mediated responses by LPS shows species variation with commensal microorganisms displaying weaker receptor binding than pathogenic species [21], a trait which enables them to form part of the normal microbiota. Species variation is also seen with the receptor-independent interactions between LPS and lipid rafts where LPS from *E. coli* binds with lower affinity to membranes than LPS from typically pathogenic species [24]. We investigated species variation in LPS-mediated response to nisin that correlates with habitation of different ecological niches. For example, lantibiotic producers are resident members of the gastrointestinal tract microbiota [51–54] and commensal Gram-negative bacteria evolving under selective pressure in their presence show reduced LPS/nisin interactions. By contrast, non-enteric pathogens that have not experienced long-term exposure to antimicrobials have LPS that confers stronger and more disruptive interactions with nisin. In the case of *B. melitensis*, a pathogen that evolved an intracellular lifestyle and characteristically multiplies in professional and non-professional phagocytes [55], LPS adaptations confer indifference to nisin as well as concealing binding sites otherwise used for recognition by antimicrobial peptides and TLR4-MD2 receptor complexes [15,42,56].

Dye release from liposomes showed that LPS from *B. melitensis* had little impact on the ability of nisin to disrupt membranes. The presence of C28 acylation in lipid A is a likely contributor to increased membrane stability and tolerance to nisin. Furthermore, the adaptations in *B. melitensis* LPS to life within a challenging ecological niche would also require low receptor binding site presentation. This was confirmed by solid state NMR, which did not show any measurable spectral changes in the presence of nisin. We did not observe the 3.2 ppm monophosphate resonances observed for deacylated core oligosaccharide [15], as most likely these monophosphates only remain after cleavage of pyrophosphates during harsh deacylation prior to solution NMR studies. Instead, we observe pyrophosphorylation, which also appears to be capped by either alkylation or with ethanolamine, which makes negative charges less accessible and can explain the more pronounced resistance of *B. melitensis* to antimicrobials. In fact, it has been shown recently that *B. melitensis* carries a lipid A phosphoethanolamine transferase gene (*lptA*) associated with resistance to polymyxin B and lipid A pyrophosphoethanolamine substitutions [49] (see also below).

LPS from the gut commensal *E. coli* and from the enteropathogenic *S. enterica* does sensitize liposomes to a slightly greater extent, which is consistent with the evolution of these organisms within the gut in a competitive environment containing natural producers of lantibiotics and other antimicrobials. Compared to *B. melitensis*, such reduction in membrane stability is likely to be augmented by the lack of C28 acylation in enterobacterial LPS. Significant phosphorylation is evident in the ^{31}P MAS NMR spectra from *E. coli* LPS, which presents binding sites for targeting by cationic antimicrobials. Indeed, major chemical shift changes confirm the existence of molecular complexes between nisin and smooth chemotype LPS from *E. coli*. Target engagement does not appear to involve directly free pyrophosphates but is mainly associated with monophosphorylated

LPS sites, suggesting the additional role of saccharides in receptor binding sites, as seen in lipid II recognition by nisin [57]. Extending the model from isolated LPS to OM extracts confirms the recognition of monophosphorylated saccharides during nisin binding to LPS.

The presence in liposomes of LPS from *K. pneumoniae* significantly increased their susceptibility to nisin in comparison to LPS from *Salmonella* and *E. coli*. As in these enteric bacteria, *Klebsiella* LPS lacks the C28 chain, which indicates that the enhanced susceptibility results from additional epitopes in the core region. Besides 1,4' lipid A phosphorylation sites [58], phosphorylation in the core region is significant and monophosphates are directly involved in the nisin binding epitope. In addition to changes in chemical shifts of monophosphates in the presence of nisin, the ^{31}P MAS NMR spectra reveal changes in dynamics in the vicinity on sugar phosphates, which suggests anchoring of the nisin/LPS complex to the membrane or the formation of a higher oligomeric state. The observed higher affinity for nisin compared to *E. coli* and *S. enterica* is likely the result of the reduced ability of *K. pneumoniae* to adapt to lantibiotic pressure in contrast to its adaptation to cationic peptides using colistin as a probe in the primary pulmonary niche [58]. While acyl chain hydroxylation under colistin pressure in murine lung infection models increases tolerance in *K. pneumoniae* [58], our results reveal a primary binding site location in the outer core of LPS such that acyl chain hydroxylation is unlikely to affect nisin/LPS interactions. Such adaptive differences reflect major differences in the molecular mechanisms of nisin and colistin and emphasize the complexity of microbial interactions in the host.

The absence of O-antigen in rough bacterial phenotypes results in LPS presenting nisin-binding sites located near the membrane surface. Solid state NMR indicates reduced population of these phosphorylation sites compared to phosphorylation in the outer core. Nonetheless, easier accessibility of these sites near the membrane markedly enhances membrane disruption by nisin.

We conclude that extensive decoy phosphorylation in the outer core underpin the protective role of LPS and resistance to antimicrobials. In agreement with this result, it has previously been shown that deletions in the core oligosaccharide lead to increased nisin sensitivity in *Salmonella typhimurium* [40].

Our results corroborate this and show that LPS from *K. pneumoniae* acts as an enhancer of nisin-induced membrane damage. It is unclear whether *K. pneumoniae* can adapt under longer term lantibiotic pressure in oxygen-rich environments *via* LpxO-mediated hydroxylation of lipid A, as observed with colistin [58,59].

The lowest levels of nisin sensitivity are seen with *E. coli, S. enterica* and *B. melitensis*. *E. coli* is a commensal bacterium which forms part of the gastrointestinal tract microbiota [60], and a low response to nisin is possibly an evolutionary adaptation based on ecological niche. Although *Salmonella* is an enteric pathogen, there are reports of *S. enterica* residing in the gastrointestinal tract in individuals who display asymptomatic carriage [61–63]. Since *S. enterica* can be recognised as a non-pathogenic resident of the gastrointestinal tract, the reduced sensitivity to nisin may also be due an evolutionary adaptation based on ecological niche. An alternative explanation is that the reduced nisin binding affinity of *S. enterica* LPS may be a protective mechanism for virulence. *Salmonella* has known antimicrobial-peptide evasion mechanisms involving structural alterations to LPS [23,64,65]. It is possible that a similar mechanism to the lipid A modification regulated by PhoPQ exists (Reference?) which protects the pathogen from the effects of nisin.

The reduced nisin sensitivity of *B. melitensis* is unusual. It has previously been shown that *Brucella* LPS is pyrophosphorylated [11] and therefore should provide a binding site for nisin. However, *Brucella* displays weak TLR4 recognition and resistance to antimicrobial peptides of the innate

immune response [6,66,67]. The lipid A moiety differs from the canonical lipid A (Figure 1) and, atypically, *B. melitensis* possesses a core oligosaccharide containing a large number of positively charged amino groups [15,56]. In this lipid A, KDO1 links lipid A to the O-antigen through a glucose unit, whilst KDO1 is linked to mannose and four glucosamine units, creating a structure that protrudes laterally, concealing the negatively charges groups essential for interaction with LPS binding proteins, CD14 and TLR4, thus evading innate immune recognition [15]. It is likely that this unusual LPS structure also provides protection against nisin. In addition to capping pyrophosphate, positive charges carried by hexosamines within the core oligosaccharide may prevent positively charged nisin from binding these concealed pyrophosphates [42,56].

The present findings show for the first time the existence of lantibiotic targets on the exterior of Gram-negative OM suggesting that lantibiotics may be used in the management of Gram-negative infections and in the control of Gram-negative food related bacteria. Phosphates in LPS within OMs are often involved in cation-mediated molecular bridges and adjuvant use of divalent cation chelators e.g. EDTA is recommended to increase their availability as nisin recognition sites. Phosphate recognition and competition with divalent cations also explains enhanced susceptibility to nisin observed in chelator-treated *E. coli* [50]. The importance of these results is enhanced by the very low frequency of resistance to nisin and the extracellular presentation of phosphates and pyrophosphates as natural receptor binding sites. Surface presentation of these chemical moieties is unique to bacteria and their function cannot be substituted by simple mutations, although further research will be required to investigate whether target modification mechanisms exist which can affect the action of lantibiotics. Using lantibiotics alone or as adjuvants in the control Gram-negative bacteria is an exciting possibility in the increasing prevalence in resistance to antibiotics.

Conclusions

The OM protects Gram-negative bacteria from environmental hazards, such as antimicrobial peptides. Structural stability in the outer leaflet is provided by *via* an electrostatic network involving phosphates and pyrophosphates on LPS bridged by divalent cations. Besides providing a protective layer and defining the chemical identity of bacteria the LPS layer presents targets for recognition by antimicrobial peptides. We investigate the role of LPS as a mediator of nisin-induced membrane damage and conclude that LPS can serve as a "receptor" for nisin and as a facilitator of nisin-induced membrane disruption. LPS from rough phenotypes, particularly the shorter type *d*, presents binding sites near the membrane surface that are readily used by nisin to destabilize the membrane. The presence of outer core and O-antigen in LPS from smooth bacterial chemotypes reveals significant phosphorylation and pyrophosphorylation, which offers decoy targets and enhances membrane resistance to antimicrobial disruption. LPS from pathogenic *K. pneumoniae* sensitizes membranes more than LPS from gut commensal *E. coli* that follows a lifestyle challenged by antimicrobials [68]. LPS from *B. melitensis*, which has evolved for a life of stealth and which has in its lipid A a long C28-OH chain, capable of traversing both membrane leaflets, has only marginal impact on membrane susceptibility to nisin. Molecular complexes readily form between nisin and LPS from pathogenic *K. pneumoniae*, as well as from gut commensal *E. coli*. The primary LPS epitope for nisin binding involves saccharide monophosphates rather than pyrophosphates that comprise the primary nisin epitopes in peptidoglycan intermediates [37]. The monophosphate targeted by nisin in smooth chemotype LPS derived from *E. coli* and reconstituted in model membranes is also targeted by nisin in *E. coli* outer membrane extracts. LPS from *B. melitensis* does not show any monophosphorylation but has an alkylated pyrophposphorylate. We saw no evidence of nisin binding, which confirms our conclusion that *B. melitensis* OM are silent and inherently resistant to nisin. We also conclude that pyrophosphate

alkylation confers additional protection against cationic antimicrobials without affecting surface charge density essential to OM stability.

Acknowledgements

The work was funded by the Biotechnology and Biological Sciences Research Council Catalyst grant BB/N010426/1. AG is co-funded by the Medical Research Council grant MR/N010477/1. AL was funded by the Wellcome Trust Antimicrobial Resistance Doctoral Training Programme (108876/Z/15/Z). CP is a BBSRC Industrial CASE Doctoral Fellow co-sponsored by DuPont Bioscience ASP, who also provided Nisaplin. Research at the Department of Microbiology and Parasitology of the University of Navarra is supported by the Institute for Tropical Health funders (Obra Social la CAIXA, Fundaciones Caja Navarra and Roviralta, PROFAND, Ubesol, ACUNSA and Artai) and by MINECO grant AGL2014-58795-CA.

REFERENCES

[1] J. O 'neill, Tackling Drug-Resistant Infections Globally: Final Report and Recommendations the Review on Antimicrobial Resistance, (2016).

[2] S. Harbarth, G. Kahlmeter, J. Kluytmans, M. Mendelson, G.S. Hospital, C. Town, S. Africa, C. Pulcini, N. Singh, U. Theuretzbacher, C.U.S. Food, S. Spring, L. Grayson, C. Houchens, D.L. Monnet, M. Ouellette, J.B. Patel, N. Zealand, E. Carrara, A. Savoldi, D. Kattula, F. Burkert, Global priority list of antibiotic-resistant bacteria to guide research, discovery, and development of new antibiotics, (2017).

[3] M.G. Gänzle, C. Hertel, W.P. Hammes, Resistance of Escherichia coli and Salmonella against nisin and curvacin A, Int. J. Food Microbiol. 48 (1999) 37–50. doi:10.1016/S0168-1605(99)00026-4.

[4] H. Nikaido, Molecular basis of bacterial outer membrane permeability revisited., Microbiol. Mol. Biol. Rev. 67 (2003) 593–656. doi:10.1128/MMBR.67.4.593.

[5] N. Ruiz, D. Kahne, T.J. Silhavy, Advances in understanding bacterial outer-membrane biogenesis., Nat. Rev. Microbiol. 4 (2006) 57–66. doi:10.1038/nrmicro1322.

[6] G.M. De Tejada, E. Moreno, I. Moriyón, The outer membranes of Brucella spp . are resistant to bactericidal cationic peptides . These include : The Outer Membranes of Brucella spp . Are Resistant to Bactericidal Cationic Peptides, Microbiology. 63 (1995) 3054–3061.

[7] C.R. Raetz, C.M. Reynolds, M.S. Trent, R.E. Bishop, Lipid A modification systems in Gram-negative bacteria, Annu. Rev. Biochem. (2007) 295–329. doi:10.1146/annurev.biochem.76.010307.145803.LIPID.

[8] C.L. Johnson, H. Ridley, R. Marchetti, A. Silipo, D.C. Griffin, L. Crawford, B. Bonev, A. Molinaro, J.H. Lakey, The antibacterial toxin colicin N binds to the inner core of lipopolysaccharide and close to its translocator protein, Mol. Microbiol. 92 (2014) 440–452. doi:10.1111/mmi.12568.

[9] E. Moreno, S.E. Stackebrandt, M. Dorsch, J. Wolters, M. Busch, H. Mayer, Brucella abortus 16S rRNA and Lipid A Reveal a Phylogenetic Relationship with Members of the Alpha-2 Subdivision of the Class Proteobacteria, J. Bacteriol. 172 (1990) 3569–3576.

[10] O. Holst, Chemical Structure of the Core Reegion of Lipopolysachharides., 1999.

[11] F. Ciesielski, D.C. Griffin, M. Rittig, I. Moriyón, B.B. Bonev, Interactions of lipopolysaccharide with lipid membranes, raft models - A solid state NMR study, Biochim. Biophys. Acta - Biomembr. 1828 (2013) 1731–1742. doi:10.1016/j.bbamem.2013.03.029.

[12] C.R. Raetz, C. Whitfield, Lipopolysaccharide endotoxins, Annu. Rev. Biochem. 71 (2002) 635–700. doi:10.1146/annurev.biochem.71.110601.135414.

[13] I. Lerouge, J. Vanderleyden, O-antigen structural variation : mechanisms and possible roles in animal / plant ^ microbe interactions, FEMS Microbiol. Rev. 26 (2001) 17–47.

[14] J. Kubler-Kielb, E. Vinogradov, W.I. Ng, B. MacZynska, A. Junka, M. Bartoszewicz, A. Zelazny, J. Bennett, R. Schneerson, The capsular polysaccharide and lipopolysaccharide structures of two carbapenem resistant Klebsiella pneumoniae outbreak isolates, Carbohydr. Res. 369 (2013) 6–9. doi:10.1016/j.carres.2012.12.018.

[15] C. Fontana, R. Conde-álvarez, J. Ståhle, O. Holst, M. Iriarte, Y. Zhao, V. Arce-gorvel, S. Hanniffy, J. Gorvel, I. Moriyón, G. Widmalm, Structural Studies of Lipopolysaccharide-defective Mutants from Brucella melitensis Identify a Core Oligosaccharide Critical in Virulence *, J. Biol. Chem. 291 (2016) 7727–7741. doi:10.1074/jbc.M115.701540.

[16] J. Kubler-Kielb, E. Vinogradov, The study of the core part and non-repeating elements of the O-antigen of Brucella lipopolysaccharide, Carbohydr. Res. 76 (2013) 33–37. doi:10.1007/s11103-011-9767-z.Plastid.

[17] E.L. Wu, O. Engstro, S. Jo, D. Stuhlsatz, M.S. Yeom, J.B. Klauda, G. Widmalm, W. Im,

Molecular Dynamics and NMR Spectroscopy Studies of E . coli Lipopolysaccharide Structure and Dynamics, 105 (2013) 1444–1455. doi:10.1016/j.bpj.2013.08.002.
[18] A. Poltorak, X. He, I. Smirnova, M.-Y. Liu, C. Van Huffel, X. Du, D. Birdwell, E. Alejos, M. Silva, C. Galanos, M. Freudenberg, P. Ricciardi-Castagnoli, B. Layton, B. Beutler, Defective LPS Signalling in C3H/HeJ and C57BL/10ScCr Mice: Mutations in TLR4 gene, Science (80-.). 282 (1998) 2085–2088.
[19] S. Akira, Mammalian Toll-like receptors, Curr. Opin. Immunol. 15 (2003) 5–11. doi:10.1016/S0952-7915(02)00013-4.
[20] J. Da Silva Correia, K. Soldau, U. Christen, P.S. Tobias, R.J. Ulevitch, Lipopolysaccharide is in close proximity to each of the proteins in its membrane receptor complex. Transfer from CD14 to TLR4 and MD-2, J. Biol. Chem. 276 (2001) 21129–21135. doi:10.1074/jbc.M009164200.
[21] S.I. Miller, R.K. Ernst, M.W. Bader, LPS, TLR4 and infectious disease diversity, Nat Rev Microbiol. 3 (2005) 36–46. doi:nrmicro1068 [pii]\r10.1038/nrmicro1068.
[22] E. Barquero-Calvo, R. Conde-Alvarez, C. Chacon-Diaz, L. Quesada-Lobo, A. Martirosyan, C. Guzman-Verri, M. Iriarte, M. Mancek-Keber, R. Jerala, J.P. Gorvel, I. Moriyon, E. Moreno, E. Chaves-Olarte, The differential interaction of Brucella and Ochrobactrum with innate immunity reveals traits related to the evolution of stealthy pathogens, PLoS One. 4 (2009) e5893. doi:10.1371/journal.pone.0005893.
[23] L. Guo, K.B. Lim, J.S. Gunn, B. Bainbridge, R.P. Darveau, M. Hackett, S.L. Miller, Regulation of Lipid A Modifications by Salmonella typhimurium Virulence genes phoP-phoQ, Science (80-.). 276 (1997) 250–253.
[24] F. Ciesielski, B. Davis, M. Rittig, B.B. Bonev, P. O'Shea, Receptor-independent interaction of bacterial lipopolysaccharide with lipid and lymphocyte membranes; the role of cholesterol, PLoS One. 7 (2012) e38677. doi:10.1371/journal.pone.0038677.
[25] J. Mares, S. Kumaran, M. Gobbo, O. Zerbe, Interactions of Lipopolysaccharide and Polymyxin Studied by NMR spectroscopy, J. Biol. Chem. 284 (2009) 11498–11506. doi:10.1074/jbc.M806587200.
[26] Y.J. Oh, B. Plochberger, M. Rechberger, P. Hinterdorfer, Characterizing the effect of polymyxin B antibiotics to lipopolysaccharide on Escherichia coli surface using atomic force microscopy, (2017) 1–7. doi:10.1002/jmr.2605.
[27] J.B. Delehanty, B.J. Johnson, T.E. Hickey, T. Pons, F.S. Ligler, Binding and Neutralization of Lipopolysaccharides by Plant Proanthocyanidins, (2007) 1718–1724.
[28] B.J. Johnson, J.B. Delehanty, B. Lin, F.S. Ligler, Immobilized Proanthocyanidins for the Capture of Bacterial Lipopolysaccharides, 80 (2008) 17112–17116.
[29] S.J. Wood, K.A. Miller, G.H. Lushington, M.R. Burns, S.A. David, Anti-Endotoxin Agents . 3 . Rapid Identification of High-Affinity Lipopolysaccharide-Binding Compounds in a Substituted Polyamine Library, (2006) 27–36.
[30] S.C. Yang, C.H. Lin, C.T. Sung, J.Y. Fang, Antibacterial activities of bacteriocins: Application in foods and pharmaceuticals, Front. Microbiol. 5 (2014) 1–15. doi:10.3389/fmicb.2014.00241.
[31] J. Dale-Skinner, B. Bonev, Molecular Mechanisms ofAntibiotic Resistance: The Need for Novel Antimicrobial Therapies, 2008.
[32] L.H. Deegan, P.D. Cotter, C. Hill, P. Ross, Bacteriocins: Biological tools for bio-preservation and shelf-life extension, Int. Dairy J. 16 (2006) 1058–1071. doi:10.1016/j.idairyj.2005.10.026.
[33] J. Delves-Broughton, Applications of the bacteriocin, nisin, Antonie van Leeuwenhoek, Int. J. Gen. Mol. Microbiol. 69 (1996) 193–202. doi:10.1007/BF00399424.
[34] B.B. Bonev, W.C. Chan, B.W. Bycroft, G.C.K. Roberts, A. Watts, Interaction of the lantibiotic nisin with mixed lipid bilayers: A P-31 and H-2 NMR study, Biochemistry. 39 (2000) 11425–

11433. doi:10.1021/bi0001170.
[35] E. Breukink, I. Wiedemann, C. van Kraaij, O.P. Kuipers, H.-G. Sahl, B. de Kruijff, Use of the Cell Wall Precursor Lipid II by a Pore-Forming Peptide Antibiotic, Science (80-.). 286 (1999) 2361–4. doi:10.1126/science.286.5448.2361.
[36] I. Wiedemann, E. Breukink, C. Van Kraaij, O.P. Kuipers, G. Bierbaum, B. De Kruijff, H.G. Sahl, Specific binding of nisin to the peptidoglycan precursor lipid II combines pore formation and inhibition of cell wall biosynthesis for potent antibiotic activity, J. Biol. Chem. 276 (2001) 1772–1779. doi:10.1074/jbc.M006770200.
[37] B.B. Bonev, E. Breukink, E. Swiezewska, B. De Kruijff, A. Watts, Targeting extracellular pyrophosphates underpins the high selectivity of nisin, FASEB J. 18 (2004). doi:10.1096/fj.04-2358com.
[38] A.J. Hyde, J. Parisot, A. McNichol, B.B. Bonev, Nisin-induced changes in Bacillus morphology suggest a paradigm of antibiotic action., Proc. Natl. Acad. Sci. U. S. A. 103 (2006) 19896–901. doi:10.1073/pnas.0608373104.
[39] A.M.S. Carneiro De Melo, G.M. Cook, R.J. Miles, R.K. Poole, Nisin stimulates oxygen consumption by Staphylococcus aureus and Escherichia coli, Appl. Environ. Microbiol. 62 (1996) 1831–1834.
[40] K.A. Stevens, N.A. Klapes, B.W. Sheldon, T.R. Klaenhammer, Antimicrobial action of nisin against Salmonella typhimurium lipopolysaccharide mutants, Appl. Environ. Microbiol. 58 (1992) 1786–1788.
[41] K.A. Stevens, B.W. Sheldon, N.A. Klapes, T.R. Klaenhammer, Nisin treatment for inactivation of Salmonella species and other gram- negative bacteria, Appl. Environ. Microbiol. 57 (1991) 3613–3615. doi:0099-2240/91/123613-03$02.00/0.
[42] J. Velasco, J.A. Bengoechea, K. Brandenburg, B. Lindner, U. Seydel, D. González, U. Zähringer, E. Moreno, I. Moriyón, Brucella abortus and its closest phylogenetic relative, Ochrobactrum spp., differ in outer membrane permeability and cationic peptide resistance, Infect. Immun. 68 (2000) 3210–3218. doi:10.1128/IAI.68.6.3210-3218.2000.
[43] J. Parisot, S. Carey, E. Breukink, W.C. Chan, A. Narbad, B. Bonev, Molecular mechanism of target recognition by subtilin, a class I lanthionine antibiotic, Antimicrob. Agents Chemother. 52 (2008) 612–618. doi:10.1128/AAC.00836-07.
[44] F. Ciesielski, D.C. Griffin, M. Rittig, B.B. Bonev, High-resolution J-coupled 13C MAS NMR spectroscopy of lipid membranes, Chem. Phys. Lipids. 161 (2009) 77–85. doi:10.1016/j.chemphyslip.2009.07.001.
[45] B.M. Fung, A.K. Khitrin, K. Ermolaev, An improved broadband decoupling sequence for liquid crystals and solids, J. Magn. Reson. 142 (2000) 97–101. doi:Doi 10.1006/Jmre.1999.1896.
[46] B.B. Bonev, Y.H. Lam, G. Anderluh, A. Watts, R.S. Norton, F. Separovict, Effects of the eukaryotic pore-forming cytolysin equinatoxin II on lipid membranes and the role of sphingomyelin, Biophys. J. 84 (2003) 2382–2392. doi:10.1016/S0006-3495(03)75044-9.
[47] W.K. Mousa, B. Athar, N.J. Merwin, N.A. Magarvey, Antibiotics and specialized metabolites from the human microbiota, Nat. Prod. Rep. 34 (2017) 1302–1331. doi:10.1039/C7NP00021A.
[48] B. Bonev, A. Watts, G. Gro, Electrostatic peptide – lipid interactions of amyloid- b peptide and pentalysine with membrane surfaces monitored by 31 P MAS NMR, (2001). doi:10.1039/b103352m.
[49] R. Conde-Álvarez, L. Palacios-Chaves, Y. Gil-Ramírez, M. Salvador-Bescós, M. Bárcena-Varela, B. Aragón-Aranda, E. Martínez-Gómez, A. Zúñiga-Ripa, M.J. de Miguel, T.L. Bartholomew, S. Hanniffy, M.-J. Grilló, M.Á. Vences-Guzmán, J.A. Bengoechea, V. Arce-Gorvel, J.-P. Gorvel, I. Moriyón, M. Iriarte, Identification of lptA, lpxE, and lpxO, Three Genes

Involved in the Remodeling of Brucella Cell Envelope, Front. Microbiol. 8 (2018) 2657. doi:10.3389/fmicb.2017.02657.
[50] J.K. Branen, P.M. Davidson, Enhancement of nisin, lysozyme, and monolaurin antimicrobial activities by ethylenediaminetetraacetic acid and lactoferrin, Int. J. Food Microbiol. 90 (2004) 63–74. doi:10.1016/S0168-1605(03)00172-7.
[51] A. Bolotin, P. Wincker, S. Mauger, O. Jaillon, K. Malarme, J. Weissenbach, S.D. Ehrlich, A. Sorokin, The Complete Genome Sequence of the Lactic Acid Bacterium, Genome Res. (2001) 731–753. doi:10.1101/gr.169701.There.
[52] L.A. David, C.F. Maurice, R.N. Carmody, D.B. Gootenberg, J.E. Button, B.E. Wolfe, A. V. Ling, A.S. Devlin, Y. Varma, M.A. Fischbach, S.B. Biddinger, R.J. Dutton, P.J. Turnbaugh, Diet rapidly and reproducibly alters the human gut microbiome, Nature. 505 (2013) 559–563. doi:10.1038/nature12820.
[53] N. Klijn, A.H. Weerkamp, W.M. De Vos, N. Klijn, A.H. Weerkamp, Genetic marking of Lactococcus lactis shows its survival in the human gastrointestinal tract . These include : Genetic Marking of Lactococcus lactis Shows Its Survival in the Human Gastrointestinal Tract, 61 (1995) 2771–2774.
[54] P. Veiga, N. Pons, A. Agrawal, R. Oozeer, D. Guyonnet, R. Brazeilles, J.-M. Faurie, J.E.T. van Hylckama Vlieg, L.A. Houghton, P.J. Whorwell, S.D. Ehrlich, S.P. Kennedy, Changes of the human gut microbiome induced by a fermented milk product, Sci. Rep. 4 (2015) 6328. doi:10.1038/srep06328.
[55] E. Barquero-Calvo, E. Chaves-Olarte, D.S. Weiss, C. Guzmán-Verri, C. Chacón-Díaz, A. Rucavado, I. Moriyón, E. Moreno, Brucella abortus uses a stealthy strategy to avoid activation of the innate immune system during the onset of infection, PLoS One. 2 (2007). doi:10.1371/journal.pone.0000631.
[56] R. Conde-Alvarez, V. Arce-gorvel, M. Iriarte, M. Mancek-Keber, E. Barquero-Calvo, L. Palacios-Chaves, C. Chacon-Diaz, E. Chaves-Olarte, A. Martirosyan, K. von Bergen, M.-J. Grillo, R. Jerala, K. Brandenburg, E. Llobert, J.A. Bengoechea, E. Moreno, I. Moriyon, J.-P. Gorvel, The Lipopolysaccharide Core of Brucella abortus Acts as a Shield Against Innate Immunity Recognition, PLOS Pathog. 8 (2012) e1002675. doi:10.1371/journal.ppat.1002675.
[57] S. Mulholland, E.R. Turpin, B.B. Bonev, J.D. Hirst, Docking and molecular dynamics simulations of the ternary complex nisin 2 :lipid II, (2016). doi:10.1038/srep21185.
[58] E. Llobet, V. Martínez-Moliner, D. Moranta, K.M. Dahlström, V. Regueiro, A. Tomás, V. Cano, C. Pérez-Gutiérrez, C.G. Frank, H. Fernández-Carrasco, J.L. Insua, T.A. Salminen, J. Garmendia, J.A. Bengoechea, Deciphering tissue-induced *Klebsiella pneumoniae* lipid A structure, Proc. Natl. Acad. Sci. 112 (2015) E6369–E6378. doi:10.1073/pnas.1508820112.
[59] A. Mularski, J. Wilksch, E. Hanssen, J. Li, T. Tomita, S.J. Pidot, T. Stinear, F. Separovic, D. Strugnell, A nanomechanical study of the effects of colistin on the Klebsiella pneumoniae AJ218 capsule, Eur. Biophys. J. 46 (2017) 351–361. doi:10.1007/s00249-016-1178-2.
[60] O. Tenaillon, D. Skurnik, B. Picard, E. Denamur, The population genetics of commensal Escherichia coli, Nat.Rev.Microbiol. 8 (2010) 207–217. doi:10.1038/nrmicro2298.
[61] J. Dekker, K. Frank, Salmonella, Shigella and Yersinia, Clin. Labortary Med. 35 (2015) 225–246. doi:10.1037/emo0000122.Do.
[62] S. Devi, C.J. Murray, Salmonella carriage rate amongst school children--a three year study., Southeast Asian J. Trop. Med. Public Health. 22 (1991) 357–361.
[63] M.B. Zaidi, J.J. Calva, M.T. Estrada-Garcia, V. Leon, G. Vazquez, G. Figueroa, E. Lopez, J. Contreras, J. Abbott, S. Zhao, P. McDermott, L. Tollefson, Integrated food chain surveillance system for Salmonella spp. in Mexico, Emerg. Infect. Dis. 14 (2008) 429–435. doi:10.3201/eid1403.071057.
[64] R.K. Ernst, T. Guina, S.I. Miller, Salmonella typhimurium outer membrane remodeling : role

in resistance to host innate immunity, (2001) 1327–1334.
[65] W.W. Navarre, T.A. Halsey, D. Walthers, J. Frye, M. McClelland, J.L. Potter, L.J. Kenney, J.S. Gunn, F.C. Fang, S.J. Libby, Co-regulation of Salmonella enterica genes required for virulence and resistance to antimicrobial peptides by SlyA and PhoP/PhoQ, Mol. Microbiol. 56 (2005) 492–508. doi:10.1111/j.1365-2958.2005.04553.x.
[66] N. Lapaque, I. Moriyon, E. Moreno, J.-P. Gorvel, Brucella lipopolysaccharide acts as a virulence factor, Curr. Opin. Microbiol. 8 (2005) 60–66.
[67] G. Tumurkhuu, N. Koide, K. Takahashi, F. Hassan, S. Islam, H. Ito, I. Mori, T. Yoshida, T. Yokochi, Characterization of biological activities of Brucella melitensis lipopolysaccharide, Microbiol Immunol. 50 (2006) 421–427. doi:JST.JSTAGE/mandi/50.421 [pii].
[68] N.H. Salzman, K. Hung, D. Haribhai, H. Chu, J. Karlsson-Sjöberg, E. Amir, P. Teggatz, M. Barman, M. Hayward, D. Eastwood, M. Stoel, Y. Zhou, E. Sodergren, G.M. Weinstock, C.L. Bevins, C.B. Williams, N.A. Bos, Enteric defensins are essential regulators of intestinal microbial ecology, Nat. Immunol. 11 (2010) 76–83. doi:10.1038/ni.1825.

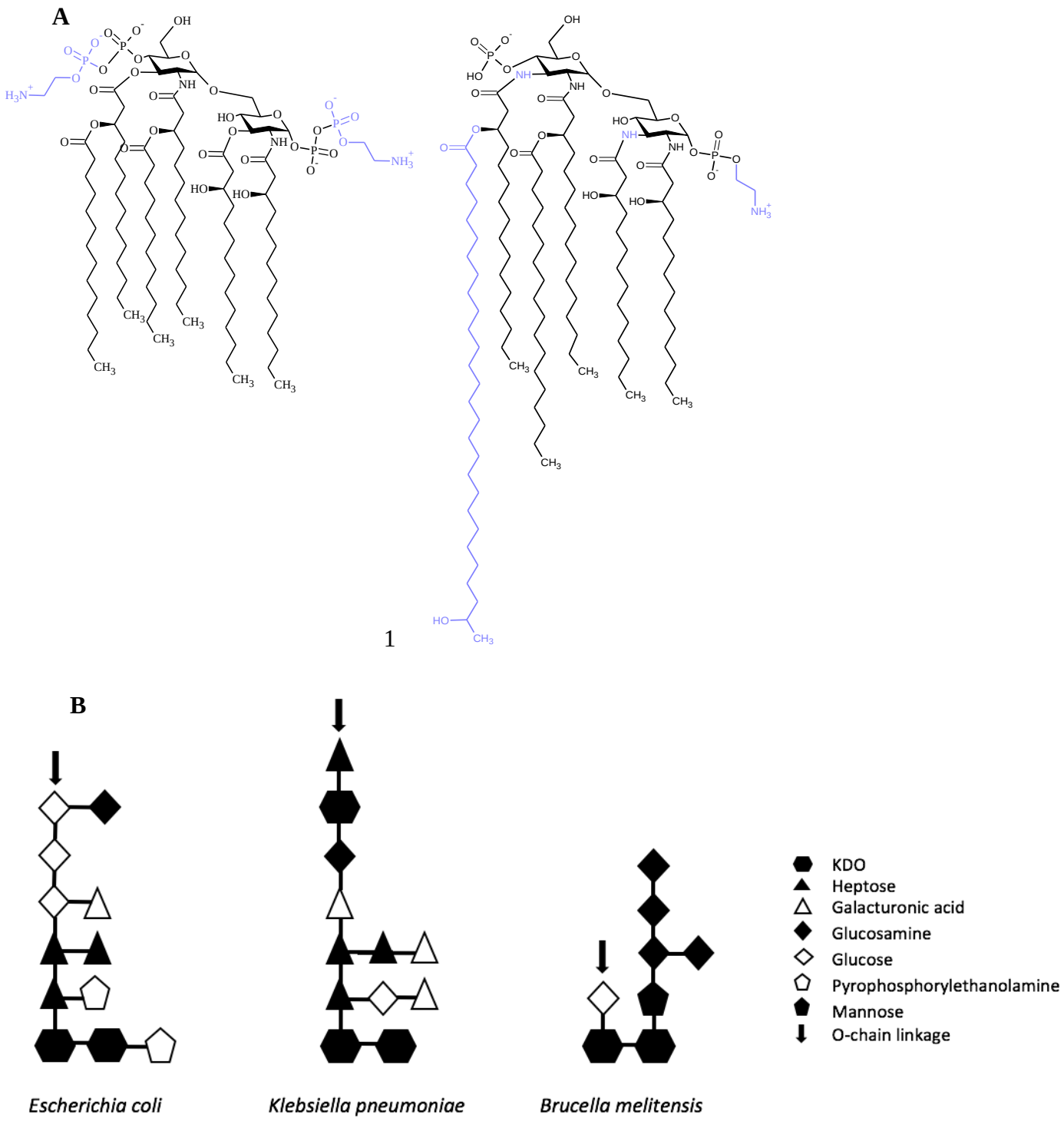

1

Figure 1: Structure and variations in bacterial LPSs:
A The structure of Lipid A in *Enterobacteriaceae* (left) and *Brucella* (right) (only the major chemical species are presented); non-canonical structures are shown in lavender. **B** Structure of the core oligosaccharides in *E. coli*, *K. pneumoniae* and *B. melitensis.*

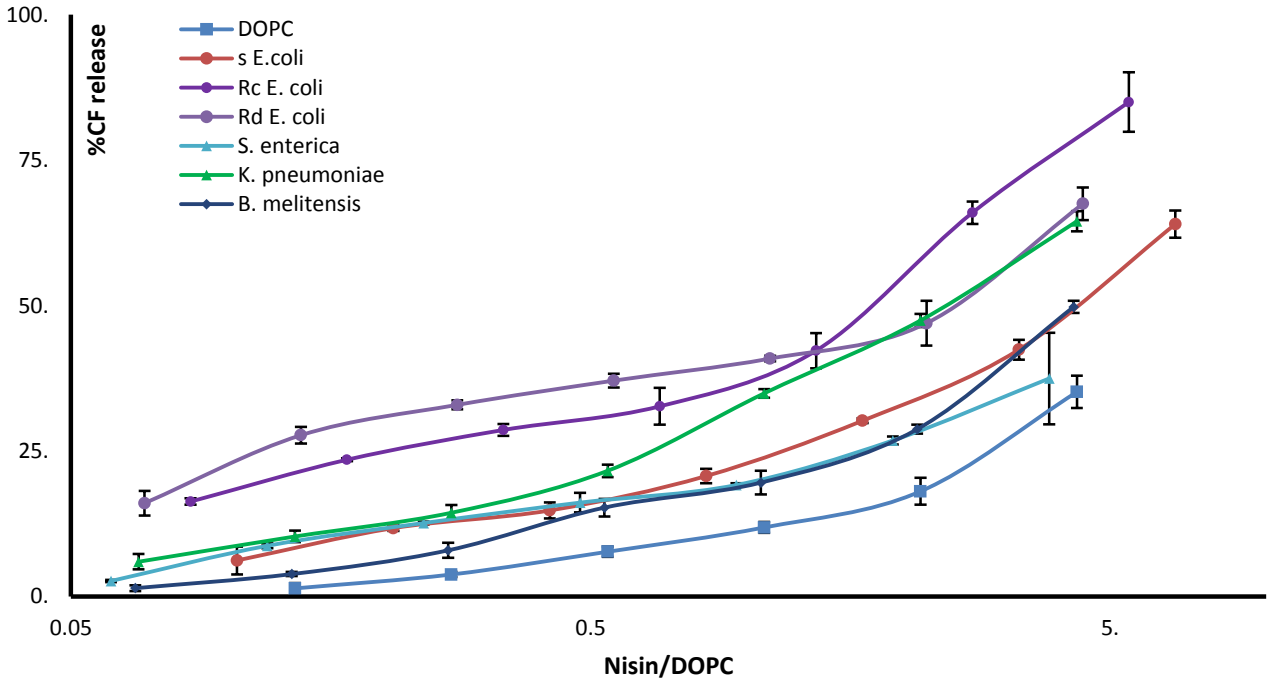

Figure 2: Nisin-mediated CF leakage

Nisin/lipid dependence of nisin-induced CF release from DOPC unilamellar vesicles alone (squares) or in the presence of 1:1 weight fraction of smooth-type LPS from *E. coli* (circles), *S. enterica* (aqua triangles), *K. pneumoniae* (green triangles) or *B. melitensis* (diamonds); or rough type c (Rc, purple) or, d (Rd, orange) from *E. coli.* Error bars show variance within the triplicate.

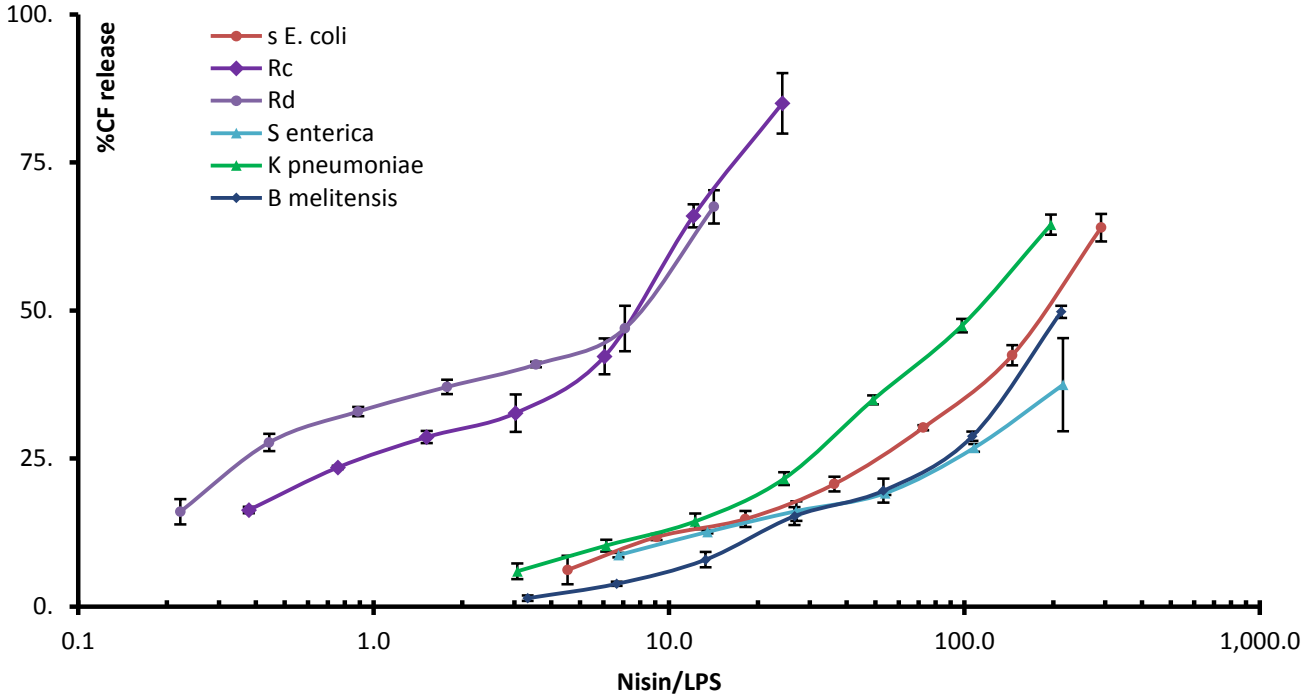

Figure 3: Dependence on LPS type of nisin-induced CF release: smooth-type LPS from *E. coli* (circles), *S. enterica* (aqua triangles), *K. pneumoniae* (green triangles), *B. melitensis* (diamonds) or, rough type c (Rc, purple) or d (Rd, orange) from *E. coli.* Error bars show variance within the triplicate.

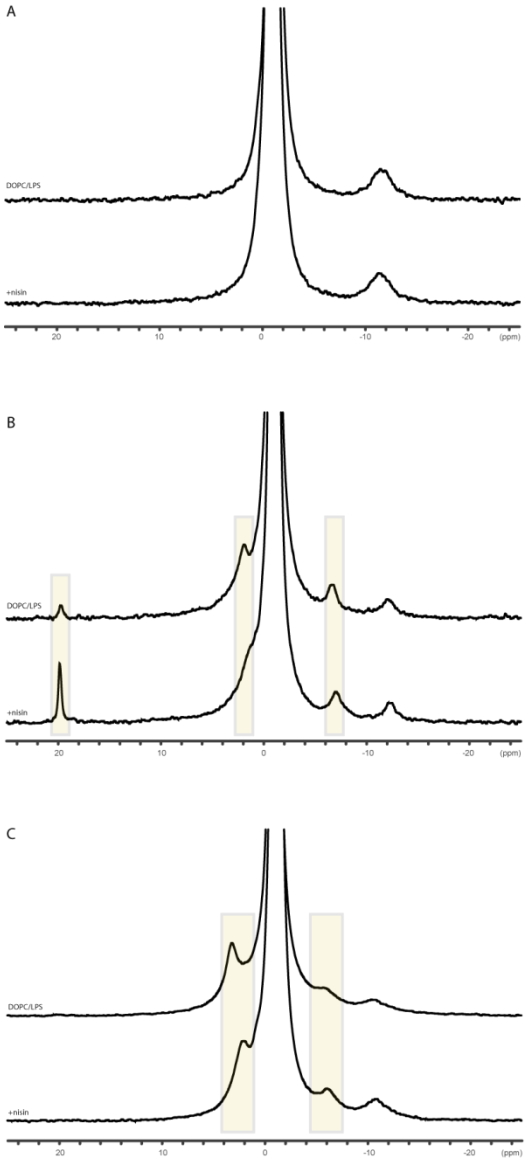

Figure 4: Direct excitation solid state ^{31}P MAS NMR spectra from DOPC MLV suspensions containing LPS from *B. melitensis* (A), *K. pneumoniae* (B) and *E. coli* smooth chemotype (C) without (top spectra) and with nisin (bottom spectra). Measurable shifts are highlighted.

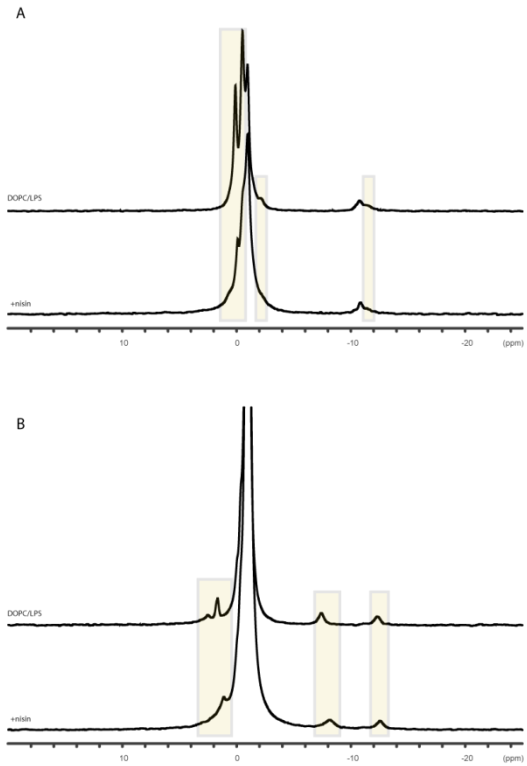

Figure 5: Direct excitation solid state ^{31}P MAS NMR spectra from DOPC MLV suspensions containing LPS from *E. coli* rough chemotype c (A) and d (B) without (top spectra) and with nisin (bottom spectra). Measurable shifts and attenuated resonances are highlighted.

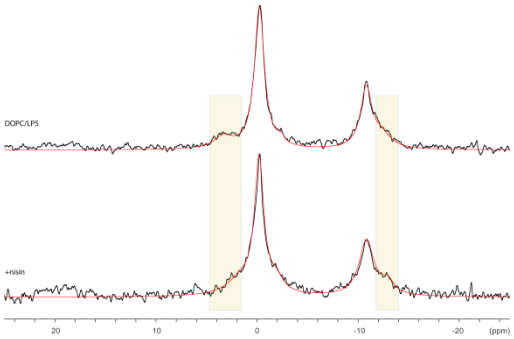

Figure 6: Direct excitation solid state ^{31}P MAS NMR spectra from *E. coli* BL21 outer membrane extracts without (top) and with nisin (bottom). Measurable shifts and attenuated resonances are highlighted. Red line shows total spectral intensity after deconvolution.